

Modeling Time-Dependent Systems using Dynamic Quantum Bayesian Networks

Sima E. Borujeni

Department of Industrial, Systems,
and Manufacturing Engineering

Wichita State University

Wichita, Kansas 67260

Email: sxborujeni@shockers.wichita.edu

Saideep Nannapaneni

Department of Industrial, Systems,
and Manufacturing Engineering

Wichita State University

Wichita, Kansas 67260

Email: saideep.nannapaneni@wichita.edu

Abstract—Advances in data collection using inexpensive sensors have enabled monitoring the performance of dynamic systems, and to implement appropriate control actions to improve their performance. Moreover, engineering systems often operate under uncertain conditions; therefore, the real-time decision-making framework should not only consider real-time sensor data processing but also several uncertainty sources that may impact the performance of dynamic systems. In this paper, we investigate the modeling of such time-dependent system behavior using a dynamic quantum Bayesian network (DQBN), which is the quantum version of a classical dynamic Bayesian network (DBN). The DBN framework has been extensively used in various domains for its ability to model stochastic relationships between random variables across time. The use of the quantum amplitude amplification algorithm provides quadratic speedup for inference and prediction in Bayesian networks. In this paper, we combine the modeling capabilities of DBN with the computational advantage of quantum amplitude amplification for efficient modeling and control of time-dependent systems. We implement the proposed DQBN framework on IBM Q hardware, and compare its performance with classical DBN implementation and the IBM Qiskit simulator.

Index Terms—Dynamic, Control, Bayesian, Quantum, Qiskit, IBM, Experimental, Circuit.

I. INTRODUCTION

Time-dependent systems are those systems whose performance characteristics change over time. A typical example of such a system is an engineering system (e.g. load-bearing structural system such as civil infrastructure [1] and aircraft system [2]) whose performance varies due to underlying mechanical degradation over time. In addition to such engineering systems, time-dependent system behavior is also observed in financial systems (stock markets) [3], healthcare (patient health management) [4], robotics [5], speech recognition [6], and bioinformatics [7]. Due to the dynamic nature of the system's performance, it becomes essential to monitor its performance in real time to ensure that the system meets the operational requirements. Early detection of any potential faults is desirable as such faults may lead to system failures leading to safety and economic consequences [8].

Such real-time system performance monitoring falls into the *digital twin* paradigm where a computer model is used as a twin to the physical system, and this computer model can be

used for real-time decision-making to minimize the effects of any failures and this improve a system's operational health [9], [10].

Engineering systems often operate under uncertain conditions; such uncertainty sources need to be identified and included in a comprehensive modeling framework [11]. In the context of structural systems, these uncertainty sources can include the variation in the load on the system, uncertainty in the material properties, and uncertainty in the amount of degradation in the system [2]. One of the widely used frameworks for modeling time-dependent systems is a Dynamic Bayesian Network (DBN), which is an extension of a Bayesian network (BN) for modeling a dynamic system. A BN has the inherent capability to represent uncertain variables, and thus, a DBN is used to represent stochastic relationships between variables over time.

Performance monitoring and fault detection is modeled as an inference problem (i.e. inferring the state of a system from observation data), and quantum algorithms have been shown to have superior computational performance over classical implementation. One of the earliest algorithms is the quantum rejection sampling algorithm, which uses the quantum amplitude amplification algorithm through the Grover's search operator [12] to achieve a quadratic speedup in the inference analysis [13], [14]. Our prior work developed a generalized discrete Quantum Bayesian network (QBN) framework on a gate-based quantum computing platform [15], and we performed an experimental evaluation of the accuracy of QBN analysis on various IBM hardware and compared their performance to the IBM Qiskit simulator and classical implementation [16].

In this paper, we develop a Dynamic Quantum Bayesian Network (DQBN) framework that integrates the computational benefits of inference analysis in QBN with the capabilities of DBN in modeling time-dependent systems for real-time system performance monitoring. We discuss the DQBN circuit representation, inference analysis, and study the solution accuracy when implemented on IBM hardware, `ibmq_16_melbourne` and the IBM Qiskit simulator against classical implementation [17].

Paper Organization: The rest of the paper is organized as follows. Section II provides a brief background to Dynamic

Bayesian networks and Quantum Bayesian networks. Section III discusses the proposed Dynamic Quantum Bayesian network framework by integrating the principles of Dynamic and Quantum Bayesian networks. Section IV discusses a case study for degradation monitoring of a structural system followed by concluding remarks in Section V.

II. BACKGROUND

A. Dynamic Bayesian Network (DBN)

A DBN falls under the state-space modeling paradigm, the state of the system is modeled using a set of unobservable ‘state’ variables, which are inferred through data available on a set of ‘observation’ variables. For modeling through a DBN, the continuous time is discretized into discrete time steps, and the system is analyzed over these discrete time steps. Fig. 1 shows a schematic of a DBN for modeling time-dependent systems.

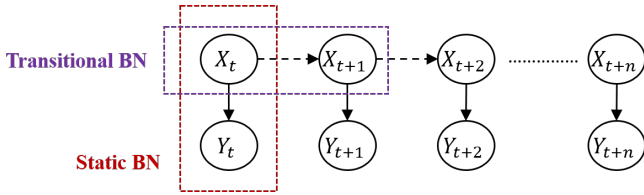


Fig. 1. A schematic of a DBN for modeling time-dependent systems

In Fig. 1, X_t and Y_t are state and observation variable at time step t . Following our previous work, we consider a DBN as a composition of two BN: (1) a static BN that models the stochastic relationships between variables in the same time step, and (2) a transitional BN that models stochastic relationships across two consecutive time steps. Fig. 1 shows temporal relationships between the state variables (dashed arrows) and relationships within the same time steps are represented using solid arrows. Here, the temporal relationships are present between two consecutive time steps only (also referred to as Markov property); this is commonly assumed when modeling using a DBN [18]. The conditional probabilities in the static and transitional BNs ($P(Y_t|X_t)$ and $P(X_{t+1}|X_t)$) remain the same and do not change over time.

Analysis using a DBN: Given data on Y_t , we obtain the posterior probabilities of X_t at time t through Bayesian inference analysis using the static BN. Using the posterior probabilities of X_t , we obtain the prior probabilities of state variables at time $t + 1$ (i.e. X_{t+1}) using the transitional BN.

B. Quantum Bayesian Network (QBN)

In this section, we provide a brief description regarding gate-based circuit representation of quantum Bayesian networks (QBNs). Here, we discuss the Compositional Quantum Bayesian Network (C-QBN) approach developed as our prior work [15] to represent any generic discrete QBN. We follow three steps for QBN circuit representation.

The first step is map each variable in a BN to one or more qubits. A qubit can be in two states. If a random variable in a

BN has more than two states, then multiple qubits need to be used to represent a BN variable. If n_s represents the number of random variable states, then the number of qubits required can be calculated as $n_q = \lceil \log_2 n_s \rceil$.

In the second step, we map the marginal and conditional probabilities of various nodes in a BN to probability amplitudes of corresponding qubits. Finally, the desired probabilities are realized by implementing (controlled) rotation gates. In the C-QBN approach, a quantum circuit is obtained by composing different blocks of gates, each block of gates correspond to realizing marginal/conditional probabilities associated with a BN variable.

For illustration, let us consider the static BN at time t in Fig. 1, which has two variables X_t and Y_t . Let us assume that each of X_t and Y_t has two states. Since they have two states, we use one qubit to represent each of them. Let $X_t = 0, 1$ and $Y_t = 0, 1$ represent the two states of X_t and Y_t . The 0 and 1 states are mapped to $|0\rangle$ and $|1\rangle$ states of their respective qubits. Fig. 2 shows the QBN circuit for the static BN with X_t and Y_t .

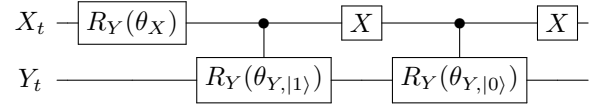


Fig. 2. A Quantum Bayesian network circuit with two nodes (qubits)

First, we implement a rotation gate (R_Y) to realize the marginal probabilities of X_t . With the implementation of $R_Y(\theta_X)$ gate, a qubit in an initial state of $|0\rangle$ gets transformed to $|0\rangle \rightarrow \cos(\frac{\theta_X}{2})|0\rangle + \sin(\frac{\theta_X}{2})|1\rangle$ with $\cos^2(\frac{\theta_X}{2})$ and $\sin^2(\frac{\theta_X}{2})$ being the probabilities of $|0\rangle$ and $|1\rangle$ states respectively. Thus the value of the rotation angle can be calculated as $\theta_X = 2 \arctan\left(\sqrt{\frac{P(X_t=1)}{P(X_t=0)}}\right)$.

Since Y_t is a child node of X_t , we have a set of probabilities for Y_t conditioned on the value of X_t . These conditional probabilities are realized through controlled rotation gates. $\theta_{Y,|1}$ and $\theta_{Y,|0}$ represent the rotation angles that need to be implemented to realize the conditional probabilities associated with $X_t = 1$ and $X_t = 0$ respectively.

When a variable in a BN has more than two states we need more than one qubit to represent it in the circuit. In that case instead of applying a single-qubit rotation, a transformation U is applied on the set of qubits for that variable.

Inside that gate U , proper rotations will transform the qubits to obtain desirable probabilities. Fig. 3 illustrates such a situation if variable X_t had more than two states. In such a case, U needs to be decomposed into a set of single qubit and CNOT basis gates. We adopt the sequential decomposition approach that was developed by Borujeni et al [15] to represent a variable with more than two states.

III. DYNAMIC QUANTUM BAYESIAN NETWORK (DQBN)

Let X_1, X_2, \dots, X_m and Y be the set of state variables and Y is an observation variable. Let $X_{1,t}, X_{2,t}, \dots, X_{m,t}$ and Y_t be the state and observation variables at time t . As mentioned

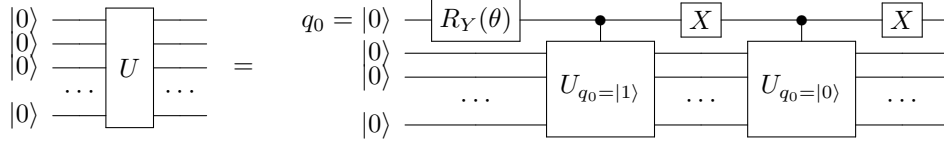


Fig. 3. Decomposition of U gate implemented on multiple qubits to represent a variable with more than two states

in section II, we consider that the Markov assumption holds good for our DBN, meaning that the state variables in each time step, only depend on their state in the previous time step. This leads us to a two time step DBN as shown in Fig. 4.

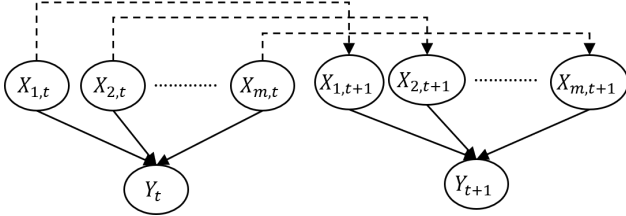


Fig. 4. A dynamic Bayesian network for a node with m parents

Following the notation in Fig. 1, the dashed arrows represent the temporal relationships (between $X_{i,t}$ and $X_{i,t+1}$, $i = 1, 2, \dots, m$) while the solids arrows represent (between $X_{i,t}$ and Y_t) relationships within the same time step. We first discuss below the analysis steps performed using a DBN, and later we present the equivalent quantum analysis.

Step 1: Given the static BN at time t (including the marginal prior probabilities of $X_{i,t}$ and conditional probability table of Y_t), we obtain the posterior probabilities of $X_{i,t}$ through Bayesian inference analysis using observation data on Y_t .

Step 2: Using the posterior probabilities of $X_{i,t}$, we obtain the prior probabilities of $X_{i,t+1}$ by performing forward prediction using the temporal conditional probabilities in the transitional BNs. Note that in the case, there are m transitional BNs, one corresponding to each $X_{i,t}$. As these m transitional BNs are independent to each other, these analyses can be performed in parallel.

We discuss below the above two steps on the quantum computing framework.

QStep 1: Before performing the Bayesian inference analysis, we need to obtain the circuit representation of the static BN. Following the discussion in Section II-B, we briefly discuss the representation of the static BN.

Static BN representation: Let A denote the quantum circuit that represents our BN and $|\psi_0\rangle$ be the state of the system after applying the unitary operator A on the qubits.

$$|0^{\otimes(m+1)}\rangle \xrightarrow{A} \text{[Circuit]} = |\psi_0\rangle \quad (1)$$

The circuit for the static BN in Fig.4 within one time step, contains m , R_Y rotations for $X_{1,t}, X_{2,t}, \dots, X_{m,t}$ and the number of different combinations of their states identifies the number of controlled rotations to be implemented to realize the conditional probabilities associates with Y_t . For a special case where all the variables are binary, A contains $2^m C^m R_Y$

rotations (with m control qubits and one target qubit). The implementation of $C^m R_Y$ when $m \geq 2$ requires $m-1$ ancilla qubits [15].

Fig. 5 shows the circuit for a simple case of $m = 2$ for binary variables $X_{1,t}, X_{2,t}$ and Y_t . In this circuit, R_{Y1} and R_{Y2} are applied for marginals and the rest of the circuit is composed of 4 section contains CCR_Y rotations for the four possible combinations of $X_{1,t}$ and $X_{2,t}$ i.e. $|00\rangle, |01\rangle, |10\rangle$ and $|11\rangle$. This whole circuit as shown inside the dashed box represents unitary operator A .

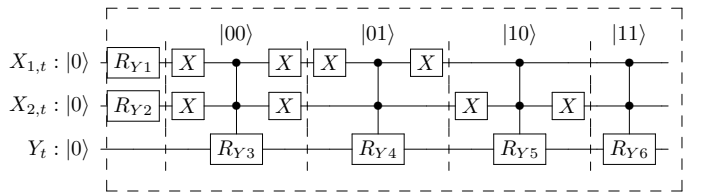


Fig. 5. Illustrative QBN with three binary variables (two state variables and one observation variable)

Bayesian inference: The estimation of posterior probabilities through Bayesian inference is carried out using the quantum amplitude amplification algorithms through Grover's operator. The posterior probabilities can be calculated as

$$\begin{aligned} P(X_{1,t}, X_{2,t}, \dots, X_{m,t} | Y_t = y_t) &= \frac{P(X_{1,t}, X_{2,t}, \dots, X_{m,t}, Y_t = y_t)}{\sum_{X_{1,t}, X_{2,t}, \dots, X_{m,t}} P(X_{1,t}, X_{2,t}, \dots, X_{m,t}, Y_t = y_t)} \quad (2) \\ &= \frac{n(X_{1,t}, X_{2,t}, \dots, X_{m,t}, Y_t = y_t)}{\sum_{X_{1,t}, X_{2,t}, \dots, X_{m,t}} n(X_{1,t}, X_{2,t}, \dots, X_{m,t}, Y_t = y_t)} \end{aligned}$$

In Eq. 2, y_t is the observation data point available on Y_t . $P(\cdot)$ is the probability function while $n(\cdot)$ represents the function that provides the counts of a state. Here, the Grover's operator for amplitude amplification is shown in Eq. 3 [14].

$$G = S_e A^\dagger S_0 A \quad (3)$$

In Eq. 3, G denotes the Grover's operator, A is the QBN circuit (corresponding to the static BN), S_0 is the zero phase shift (reflection operator), A^\dagger is the conjugate transpose of A , and S_e is the phase oracle defined below in Eq. 4.

$$\begin{aligned} S_e : |x\rangle &\rightarrow (-1)^{f(x)} |x\rangle, \text{ where :} \\ f(x) &= \begin{cases} 1, & \text{if } x \text{ is a good state} \\ 0, & \text{otherwise} \end{cases} \quad (4) \end{aligned}$$

In Eq. 4, $|x\rangle$ correspond to a quantum state in the QBN circuit. Combining Eq. 1 with the Grover operator (Eq. 3), we have

$$|0^{\otimes(m+1)}\rangle \xrightarrow{A} \xrightarrow{G} \quad (5)$$

or

$$|\psi_0\rangle \xrightarrow{S_e} \xrightarrow{A^\dagger} \xrightarrow{S_0} \xrightarrow{A} \xrightarrow{\text{Measurement}} = |\psi_1\rangle \quad (6)$$

The Grover operator here, amplifies the probabilities of the good states, which in our case, are the states that are inferred. Depending on the number of good states, we implement multiple Grover iterations as shown in Eq. 7.

$$|\psi_0\rangle \xrightarrow{\text{k iterations}} \left[\xrightarrow{S_e} \xrightarrow{A^\dagger} \xrightarrow{S_0} \xrightarrow{A} \right] \xrightarrow{\text{Measurement}} = |\psi_k\rangle \quad (7)$$

QStep 2: After obtaining the posterior probabilities of the state variables, we calculate their prior probabilities in the next time step using the transitional BN. In Fig 4, we have m transitional BNs, one corresponding to each $X_{i,t}$. Fig. 6 shows the quantum circuit of a transitional BN.

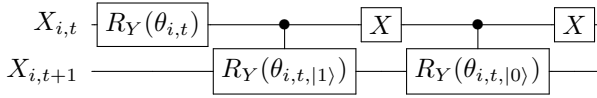


Fig. 6. Illustrative transitional QBN of a state variable over two time steps

In Fig. 6, $\theta_{i,t}$ is the rotation angle that corresponds to the posterior probabilities of $X_{i,t}$, and $\theta_{i,t,|1}$ and $\theta_{i,t,|0}$ correspond to the rotation angles to be implemented to realize the probabilities of $X_{i,t+1}$ when conditioned on $X_{i,t} = 1$ and $X_{i,t} = 0$. It should be noted that the prior probabilities of $X_{i,t+1}$ can be obtained by simulating the transitional QBN without any need for Grover operators and inference analysis.

Since the conditional probabilities in the static and transitional BNs remain the same across multiple time steps, the architectures of the static and transitional QBNs (in Figs. 5,6) also remain the same. In both the QBN circuits, the rotation angles associated with the marginal probabilities vary over time (e.g. $\theta_{i,t}$ in Fig. 6; R_{Y1} and R_{Y2} in Fig. 5).

IV. CASE STUDY, RESULTS, AND DISCUSSION

In this section, we demonstrate the proposed DQBN approach for health monitoring of a simulated structural system, where X_t and Y_t represent the load and response of a structural system respectively. In addition to the load, the response also depends on any structural degradation (e.g. cracks); this is denoted as d_t . The motivation for this example was derived from work done by Bartram [19] and Li et al [2], where DBNs were used for health management and prognostics of mechanical and aerospace systems respectively. The DBN of this example is given in Fig. 7.

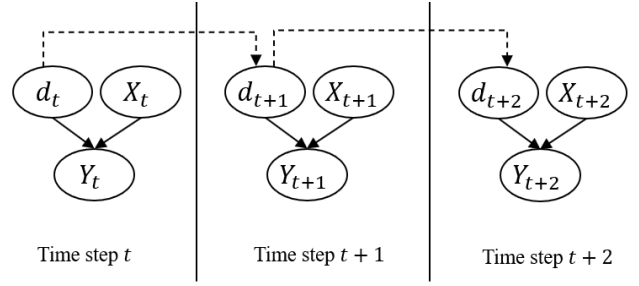


Fig. 7. The dynamic Bayesian network with 3nodes over three time steps

Both the load and response variables (X_t, Y_t) are discretized into three levels - {Low, Medium, High} and denoted as $\{0, 1, 2\}$. The deterioration variable d_t is discretized into two levels - {Minor, Major} and denoted as $\{0, 1\}$ respectively. The marginal probabilities of d_t at time $t = 0$ are given as $P(d_0 = 0) = 0.95$ and $P(d_0 = 1) = 0.05$. Similarly, the probabilities of X_t at time $t = 0$ are given as $P(X_0 = 0) = 0.2$, $P(X_0 = 1) = 0.5$ and $P(X_0 = 2) = 0.3$. The probabilities of Y_t conditioned on d_t and X_t are given in Table I.

TABLE I
CONDITIONAL PROBABILITIES OF RESPONSE DEPENDENT OF DEGRADATION AND LOAD

	(0,0)	(0,1)	(0,2)	(1,0)	(1,1)	(1,2)
$P(Y_t = 0 d_t, X_t)$	0.8	0.75	0.65	0.15	0.05	0
$P(Y_t = 1 d_t, X_t)$	0.15	0.18	0.23	0.55	0.6	0.35
$P(Y_t = 2 d_t, X_t)$	0.05	0.07	0.12	0.3	0.35	0.65

Engineering systems age and their performance naturally degrades over time. Here, the degradation is modeled through a transitional conditional probability distribution across two steps following the Markov property, i.e., the degradation in the current time step is dependent on the degradation in the previous time step. The conditional distribution of d_{t+1} dependent on d_t is given in Table II.

TABLE II
CONDITIONAL PROBABILITY RELATIONSHIP OF DEGRADATION ACROSS TWO TIME STEPS

	$d_t = 0$	$d_t = 1$
$P(d_{t+1} = 0)$	0.9	0
$P(d_{t+1} = 1)$	0.1	1

- We perform two types of analysis through this case study.
- 1) Track probability distribution of degradation over time
 - 2) Compare the solution accuracy between classical analysis, IBM Qiskit simulator and IBM Q hardware.

Modeling DQBN: As discussed in Section III, we decompose the DBN into two BNs: (1) Static BN, and (2) Transitional BN. We model the joint distribution between d_t, X_t and Y_t through the static BN at each time step, and we model the joint distribution between the degradation variables across two consecutive time steps. Here, we first discuss the circuit representations of static and transitional BNs at time $t = 0$.

Static BN at time $t = 0$: A schematic representation of the static BN is shown in Fig. 8. Since X_t and Y_t each has three levels, we use two qubits to represent each of these two variables. We use one qubit to represent the two levels of d_t , totaling to five qubits.

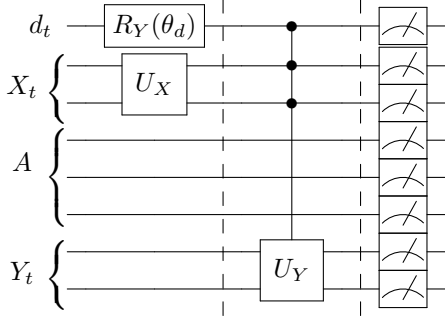


Fig. 8. Schematic of the static BN

Since $P(d_0 = 0) = 0.95$ and $P(d_0 = 1) = 0.05$, the rotation angle to be implemented to realize these probabilities can be calculated as $\theta_d = 2 \arctan\left(\sqrt{\frac{P(d_0=1)}{P(d_0=0)}}\right) = 0.451$. The variable X_0 (i.e. X_t at $t = 0$) has three states 0,1, and 2. We represent these three states using two qubits. We map the three states to $|00\rangle$, $|01\rangle$, and $|10\rangle$ states respectively. As discussed in Section II, we decompose the two-qubit U_X gate into a set of single qubit and CNOT gates shown in Fig. 9.

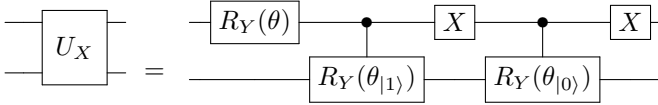


Fig. 9. Circuit representation of a two-qubit gate using single qubit and controlled rotations

In Fig. 9, $R_Y(\theta)$ is the single-qubit rotation gate implemented on the first qubit, $\theta_{|1}$ and $\theta_{|0}$ are the conditional rotation angles implemented on the second qubit with the first qubit as the control qubit. Here, $\theta = 2 \arctan\left(\sqrt{\frac{P(|10\rangle)+P(|11\rangle)}{P(|00\rangle)+P(|01\rangle)}}\right) = 1.159$. Similarly, $\theta_{|1}$ and $\theta_{|0}$ can be calculated as $\theta_{|1} = 2 \arctan\left(\sqrt{\frac{P(|11\rangle)}{P(|10\rangle)}}\right) = 0$ and $\theta_{|0} = 2 \arctan\left(\sqrt{\frac{P(|01\rangle)}{P(|00\rangle)}}\right) = 2.014$. Depending on the values of d_t and X_t , we have several conditional probabilities as given in Table I, which are represented using conditional rotations over two qubits (shown in Fig. 8). As there are six combinations of d_t and X_t , we will have six different U_Y gates.

Similar to U_X , U_Y can also be decomposed into single qubit and controlled rotation gates. As shown in Fig. 8, we need to implement three-qubit (one d_t and two of X_t) controlled rotation over two qubits in order to realize the conditional probabilities of Y_t . Decomposition of U_Y itself requires a controlled rotation; therefore, implementation of C^3U_Y gate requires four-qubit (three for d_t and X_t , and one for decomposition of U_Y as shown in Fig. 9) controlled

rotation. We use three ancilla qubits to realize the four-qubit controlled rotation. In total, the circuit requires eight qubits; five qubits to represent the three variables and three ancilla qubits to implement the controlled rotation gates.

It should be noted that the rotation angle θ_d changes at each time step and the rest of the static BN remains the same. Note that the marginal probabilities of X_t are do not change with time. Therefore, we can use the same static BN (with the change in θ_d) in each time step without the need to construct a different static BN circuit at each time step.

Transitional BN across two time steps: A schematic representation of the transitional BN with degradation variables across two consecutive time steps is given in Fig. 10.

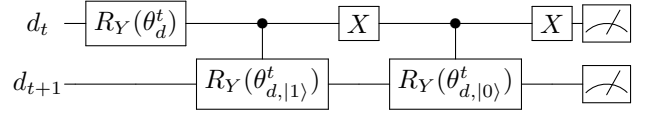


Fig. 10. Schematic of the transitional BN across two consecutive steps

In Fig. 10, θ_d^t represents the angle to realize the posterior probabilities of d_t (and not the prior probabilities). The posterior probabilities can be obtained using data on Y_t and the quantum amplitude amplification algorithm. Using the posterior probabilities of d_t at time step t , we calculate the prior probabilities of d_t at time $t+1$. In Fig. 10, $\theta_{d,|1}^t$ and $\theta_{d,|0}^t$ are rotation angles associated with the conditional probabilities of d_{t+1} when $d_t = 1$ and $d_t = 0$ respectively. Similar to the static BN circuit, the transitional BN circuit does not change except for the change in θ_d^t as the transitional conditional probabilities remain the same across any two time steps.

Degradation estimation: So far, we discussed about the circuit representation of static and transitional BNs. Here, we will discuss the estimation of state variable (degradation; d_t) using data on observation variables (response variables Y_t and X_t). We will demonstrate the proposed framework for five time steps. The observation data of Y_t across these five steps is assumed as $\{0, 1, 1, 1, 2\}$. We also consider the observation data for X_t at these five time steps as $\{1,0,2,1,2\}$. In the first time step, the observation of Y_t is 0 and the observation of X_t is 1. As discussed, $Y_t = 0$ is represented using two qubits as $|00\rangle$ and $X_t = 1$ would be $|01\rangle$. For posterior distribution of d_t , we need to calculate $P(d_t = 0|Y_t = 0, X_t = 1)$ and $P(d_t = 1|Y_t = 0, X_t = 1)$.

The estimation of degradation variable through quantum amplification requires us to build an Oracle. In the Oracle, we fix the two qubits related to Y_t at $|0\rangle$ (resulting in $|00\rangle$ state), fix the two qubits related to X_t at $|0\rangle$ and $|1\rangle$ respectively (resulting in $|01\rangle$ state) and the three ancilla qubits at $|0\rangle$ state. Ideally, the ancilla qubits should be in $|0\rangle$; however, the presence of experimental noise cause the ancilla qubits to not be in the exact $|0\rangle$ states. Fixing the ancilla qubits at $|0\rangle$ results in a more effective estimation of the state (degradation) variable. Using this oracle, we implement the Grover rotations to calculate the posterior probabilities of d_t .

Of the eight qubits, we fix the values of seven qubits (two relating to Y_t , two relating to X_t and three ancilla qubits) while the remaining qubit can either be in $|0\rangle$ or $|1\rangle$ state. We ran the analysis with 8192 shots and obtain the number of counts when the qubit associated with d_t is in $|0\rangle$ and $|1\rangle$ states. If n_0 and n_1 represent the amount of such counts, then the posterior probabilities can be calculated as $P(d_t = 0|Y_t = 0, X_t = 1) = \frac{n_0}{n_0+n_1}$ and $P(d_t = 1|Y_t = 0, X_t = 1) = \frac{n_1}{n_0+n_1}$. Three iterations of Grover’s operator can give us the optimal solution while adding more iterations worsens the results. These posterior probabilities are then used to calculate the prior probabilities in the next time step using the transitional BN circuit in Fig. 10.

Discussion: The results of the DQBN analysis are provided in Fig.11. The three bar plots provide the prior and posterior probabilities of degradation variable d_t across five time steps. It could be observed that the qasm_simulator results closely match the classical results (through Netica software [20]). The root mean squared (RMS) error in the prior and posterior probabilities of $d_t = 0$ between Qiskit simulator and classical implementation is calculated as 1.192%. The RMS error for IBM Melbourne is equal to 34.66%. We believe the discrepancy in the results between IBM hardware and Qiskit simulator is due to the inherent hardware (gate) errors, decoherence, and the large depth of the circuits. For example, the depth of the *transpiled* static QBN circuit at time $t = 0$ is 946. Even though the static BN has three variables d_t , X_t and Y_t , the QBN representation required eight qubits (including three ancilla qubits) and contained 769 CNOT gates. This is the reason for the larger depth of the transpiled circuit.

V. CONCLUSION

This paper described state-space modeling of time-dependent systems using Dynamic Quantum Bayesian networks (DQBN). DQBN are extensions of Quantum Bayesian networks (QBNs) for modeling dynamic systems. We considered a DQBN as a composition of two QBNs: a static QBN that describes the relationships between variables at any given time, and a transitional QBN that describes the relationships between variables across two consecutive time steps. At any given time step, the posterior probabilities of unobserved state variables are estimated using data on observation variables using quantum amplitude amplification algorithms through Grover iterations. The posterior probabilities of the state variables are then used to obtain their prior probabilities in the next time step through transitional QBN simulation. In this way, through repeated evaluation of static and transitional QBNs, we can track the performance of time-dependent systems. This paper demonstrated the proposed framework for degradation monitoring of a structural system. We performed the analysis on the IBM Qiskit simulator and IBM hardware and compared their performance against classical implementation (through Netica software). We observed that the IBM simulator results were close to the classical results whereas the results from IBM hardware (Melbourne device) were error-prone, noisy, and therefore, unreliable.

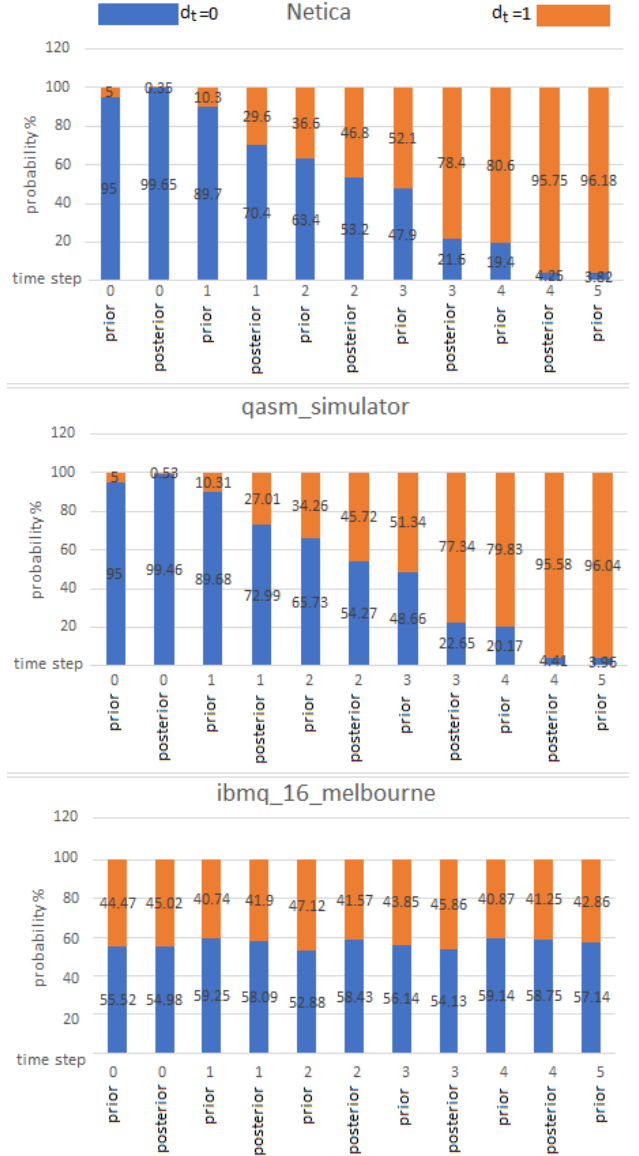


Fig. 11. Prior and posterior distribution of d_t over five consecutive time steps using Netica, qasm_simulator, and ibmq_16_melbourne

As future work, we will investigate the scalability of the proposed framework for high-dimensional systems (increasing the number of variables and increasing the number of states of each variable). Moreover, we will also incorporate gate and measurement error mitigation strategies to improve the solution performance on the IBM hardware. We will also investigate other quantum inference algorithms for state estimation such as quantum Metropolis algorithm [21] and variational inference methods [22].

ACKNOWLEDGEMENT

We acknowledge the use of IBM Quantum services for this work. The views expressed are those of the authors, and do not reflect the official policy or position of IBM or the IBM Quantum team.

REFERENCES

- [1] J. Luque and D. Straub, "Risk-based optimal inspection strategies for structural systems using dynamic bayesian networks," *Structural Safety*, vol. 76, pp. 68–80, 2019.
- [2] C. Li, S. Mahadevan, Y. Ling, S. Choze, and L. Wang, "Dynamic bayesian network for aircraft wing health monitoring digital twin," *Aiaa Journal*, vol. 55, no. 3, pp. 930–941, 2017.
- [3] Y. Liu, Y. Wang, G. Zheng, J. Wang, and K. Guo, "The dynamical relationship between capital market and macroeconomy: based on dynamic bayesian network," *Procedia Computer Science*, vol. 162, pp. 46–52, 2019.
- [4] M. A. Van Gerven, B. G. Taal, and P. J. Lucas, "Dynamic bayesian networks as prognostic models for clinical patient management," *Journal of biomedical informatics*, vol. 41, no. 4, pp. 515–529, 2008.
- [5] C. Premebida, D. R. Faria, and U. Nunes, "Dynamic bayesian network for semantic place classification in mobile robotics," *Autonomous Robots*, vol. 41, no. 5, pp. 1161–1172, 2017.
- [6] A. V. Nefian, L. Liang, X. Pi, X. Liu, and K. Murphy, "Dynamic bayesian networks for audio-visual speech recognition," *EURASIP Journal on Advances in Signal Processing*, vol. 2002, no. 11, pp. 1–15, 2002.
- [7] M. Zou and S. D. Conzen, "A new dynamic bayesian network (dbn) approach for identifying gene regulatory networks from time course microarray data," *Bioinformatics*, vol. 21, no. 1, pp. 71–79, 2005.
- [8] Y. Jiang, S. Yin, and O. Kaynak, "Data-driven monitoring and safety control of industrial cyber-physical systems: Basics and beyond," *IEEE Access*, vol. 6, pp. 47 374–47 384, 2018.
- [9] E. VanDerHorn and S. Mahadevan, "Digital twin: Generalization, characterization and implementation," *Decision Support Systems*, p. 113524, 2021.
- [10] M. G. Kapteyn and K. E. Willcox, "From physics-based models to predictive digital twins via interpretable machine learning," *arXiv preprint arXiv:2004.11356*, 2020.
- [11] S. Nannapaneni, Z. Hu, and S. Mahadevan, "Uncertainty quantification in reliability estimation with limit state surrogates," *Structural and Multidisciplinary Optimization*, vol. 54, no. 6, pp. 1509–1526, 2016.
- [12] L. K. Grover, "A fast quantum mechanical algorithm for database search," in *Proceedings of the twenty-eighth annual ACM symposium on Theory of computing*, 1996, pp. 212–219.
- [13] M. Ozols, M. Roetteler, and J. Roland, "Quantum rejection sampling," *ACM Transactions on Computation Theory (TOCT)*, vol. 5, no. 3, pp. 1–33, 2013.
- [14] G. H. Low, T. J. Yoder, and I. L. Chuang, "Quantum inference on bayesian networks," *Physical Review A*, vol. 89, no. 6, p. 062315, 2014.
- [15] S. E. Borujeni, S. Nannapaneni, N. H. Nguyen, E. C. Behrman, and J. E. Steck, "Quantum circuit representation of bayesian networks," *Expert Systems with Applications*, vol. 176, p. 114768, 2021.
- [16] S. E. Borujeni, N. H. Nguyen, S. Nannapaneni, E. C. Behrman, and J. E. Steck, "Experimental evaluation of quantum bayesian networks on ibm qx hardware," in *2020 IEEE International Conference on Quantum Computing and Engineering (QCE)*. IEEE, 2020, pp. 372–378.
- [17] IBM, "Ibm quantum," <https://quantum-computing.ibm.com/>, June 2021.
- [18] K. P. Murphy, "Dynamic bayesian networks: representation, inference and learning," Ph.D. dissertation, University of California, Berkeley Berkeley, CA, 2002.
- [19] G. W. Bartram, "System health diagnosis and prognosis using dynamic bayesian networks," Ph.D. dissertation, Vanderbilt University, 2013.
- [20] Netica, "Norsys software corporation, netica version 6.05," <https://www.norsys.com/>, 2019.
- [21] K. Temme, T. J. Osborne, K. G. Vollbrecht, D. Poulin, and F. Verstraete, "Quantum metropolis sampling," *Nature*, vol. 471, no. 7336, pp. 87–90, 2011.
- [22] M. Benedetti, B. Coyle, M. Fiorentini, M. Lubasch, and M. Rosenkranz, "Variational inference with a quantum computer," *arXiv preprint arXiv:2103.06720*, 2021.